International Journal of Solids and Structures 50 (2013) 3649–3658

Contents lists available at SciVerse ScienceDirect

International Journal of Solids and Structures

journal homepage: www.elsevier.com/locate/ijsolstr

Stress concentration factor due to a functionally graded ring around a hole in an isotropic plate

Roberta Sburlati *

Department of Civil, Chemical and Environmental Engineering, DICCA, University of Genova, Via Montallegro 1, 16145 Genova, Italy

ARTICLE INFO

Article history:
Received 22 February 2013
Received in revised form 9 July 2013
Available online 19 July 2013

Keywords:
Linear elasticity theory
Functionally graded materials
Stress concentration factor
Circular hole

ABSTRACT

The aim of this work is to present an analytical solution to reduce the stress concentration factor (SCF) around a circular hole in an isotropic homogeneous plate subjected to far-field uniaxial loading. In this paper the elastic response of an inhomogeneous annular ring made of functionally graded material (FGM), inserted around a hole of a homogeneous plate, is studied. By assuming that Young's modulus varies in the radial direction with power law and that Poisson's ratio is constant, the governing differential equations for plane stress conditions are obtained. Using stress function a general solution in explicit closed form is presented and the SCF investigated to highlight the inhomogeneity effects. Furthermore, the explicit solution for an inner homogeneous ring, with different properties with respect to those of the plate, is explicitly obtained and numerical results are compared between homogeneous ring and FGM ring.

1. Introduction

Functionally graded materials (FGMs) are composites made of two or more constituent phases with a continuously variable composition. These materials are usually associated with particulate composite where the volume fraction of particles varies in one or several directions; at the macroscopic scale the composite may be assumed inhomogeneous and often locally isotropic. In view of the growing importance of these materials, an accurate investigation into elastic deformation for inhomogeneous structures is devoted to improve their performance in applications. Birman and Byrd (2007) have presented a review of the principal developments in functionally graded materials and of the diverse areas of interest of this topic for a successful implementation of these materials. The concept of FGM is used by many authors to model the interphase zone around an inclusion in periodic composite to develop homogeneization methods and determine effective elastic properties of the composite (Lutz and Zimmerman, 1996; Artioli et al., 2010; Dryden and Batra, 2013). Many authors investigate the response of FGM composite systems with different geometries such as hollow cylinders, coatings on substrate and sandwich panels to obtain benchmarks for the accuracy of numerical solutions and to provide useful information in FGM design (Batra, 2011; Theotokoglou and Tampouloglou, 2008; Hosseini-Hashemi et al., 2013; Sburlati et al., 2013).

This work deals with the problem of maximizing the strength of a homogeneous plate with a circular hole subjected to uniaxial load by using an annular ring around the hole made of FGM with properties varying in radial direction. We shall show that, with a suitable choice of the ring graded material properties, the maximum value of the hoop stress, computed on all the material regions, can be reduced with respect to the homogeneous plate value. This can be useful to prevent mechanical failure in the entire plate.

A biomimetic approach regarding the fact that blood vessel holes in load-bearing bones are not normally involved in structural failures suggested the idea of this paper. Actually, some studies have found that the increase of strength is due to a radial distribution of the elastic modulus around the holes which reduce the stress concentration factor (SCF) when compared to those in homogeneous plates (Buskirk et al., 2002; Nagpal et al., 2012). The method to reduce SCF around circular or elliptic holes applying reinforced homogeneous layers embedded in homogeneous plate has been widely used in applications; however in so doing, the interfacial mismatch-induced stresses become relevant for the mechanical integrity of the plate and an optimum design also requires reduction of interfacial stress by material combination and geometric configuration (Chao et al., 2009; Sburlati, 2009a). In a similar way, the interest of some authors is devoted to reducing the mismatch of thermo mechanical properties at the interface by using FGM to increase the resistance of film/coating to contact or impact problems (Suresh, 2001; Sburlati, 2002; Sburlati, 2004; Kashtalyan and Menshykova, 2008; Sburlati, 2012a).

* Tel.: +39 103532502; fax: +39 103532535.
E-mail address: roberta.sburlati@unige.it

0020-7683/$ - see front matter © 2013 Elsevier Ltd. All rights reserved.
http://dx.doi.org/10.1016/j.ijsolstr.2013.07.007

In recent years, researchers have studied the problem to reduce SCF around holes by using entire FGM plates. Kubair and Bhanu-Chandar (2008) have numerically investigated the effect of material inhomogeneity on the SCF due to a circular hole in functionally graded panels by using different graded laws (potential and exponential); a parametric study was performed using a finite element approach. The authors have shown that a desired reduction in the SCF is obtained when the material properties progressively increase away from the hole. On the other hand, the SCF is least affected by Poisson's ratio. A different approach was used by Yang et al. (2010) to study the two-dimensional stress distribution of a functionally graded plate with circular hole under arbitrary constant loads. By using the method of piece-wise homogeneous layers the solution was obtained by means of complex variable functions. The stress reduction was investigated and it was also found that Poisson's ratio variation influences the reduction of the SCF less. In Mohammadi et al. (2011), a radial expression of Young's modulus depending on two adjustable parameters was used. This assumption also permits us to model a plate where the FGM behavior is essentially bounded in a region around the hole. The SCF in a plate made of functionally graded material was considered by assuming Young's modulus and Poisson's ratio exponentially variable in the radial direction. In the cases of biaxial tension and pure shear load the SCF was obtained in terms of Kummer's functions and the influence of the inhomogeneity effects were investigated. We remark that most of the above mentioned studies concern entire FGM plates; however, in practice, it is often not feasible to manufacture an entire plate with graded material and it is sufficient to use only a thin FGM coating around a hole to mitigate the SCF (Sburlati, 2012b).

In this paper an analytical solution in closed form for a homogeneous plate subjected to uniaxial load with a radially functional graded ring inserted around the inner hole is obtained. To study the local effect of the hole we assume the infinite medium model for the homogeneous isotropic plate. The graded material in the thickness of the ring is considered with Young's modulus that varies with a monotonic power law; Poisson's ratio is assumed constant and equal in the ring and in the isotropic medium. This last assumption is motivated by numerical investigations concerning the entire FGM plate. Furthermore, we assume the ring and the plate perfectly connected together. The Airy stress function is introduced by plain stress conditions to obtain the explicit elastic solution in closed form (Nie and Batra, 2010; Sburlati, 2009b). Then we compare these solution with the case of a homogeneous ring. The investigation of numerical results permits us to give information on the constitutive and geometric parameters to optimize the strength of the plate by material tailoring. Maple program was used for formal calculations and numerical results.

2. Problem formulation

To analyze the local effects around the hole in a plate we assume the model of an infinite elastic medium with a circular hole of radius a subjected to a inplane uniform far-field uniaxial load P as shown in Fig. 1. The effects of two different rings around the hole ($a \leqslant r \leqslant b$) are studied: a homogeneous (HM) isotropic ring and a functionally graded (FG) ring. The plane stress assumptions are introduced and in the FGM we consider radial variation of Young's modulus and Poisson's ratio constant.

By using a cylindrical coordinate system $(0; r, \theta, z)$ the equations of equilibrium in the absence of body forces are

$$\frac{\partial \sigma_r}{\partial r} + \frac{1}{r}\frac{\partial \sigma_{r\theta}}{\partial \theta} + \frac{\sigma_r - \sigma_\theta}{r} = 0, \quad \frac{\partial \sigma_{r\theta}}{\partial r} + \frac{1}{r}\frac{\partial \sigma_\theta}{\partial \theta} + \frac{2}{r}\sigma_{r\theta} = 0, \tag{2.1}$$

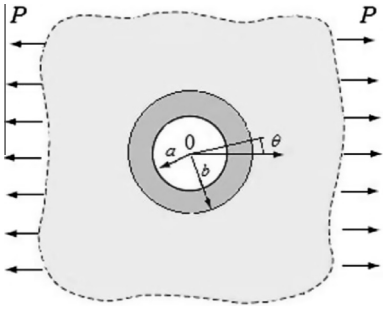

Fig. 1. Homogeneous medium subjected to a far-field uniaxial load with an FGM ring around the hole.

where $\sigma_r, \sigma_{r\theta}$ and σ_θ are the stress components. The displacement components u_r and u_θ are related to the strains $\varepsilon_r, \varepsilon_\theta$ and $\varepsilon_{r\theta}$ by

$$\varepsilon_r = \frac{\partial u_r}{\partial r}, \quad \varepsilon_\theta = \frac{u_r}{r} + \frac{1}{r}\frac{\partial u_\theta}{\partial \theta}, \quad \varepsilon_{r\theta} = \frac{1}{r}\frac{\partial u_r}{\partial \theta} + \frac{\partial u_\theta}{\partial r} - \frac{u_\theta}{r} \tag{2.2}$$

and the compatibility equation is

$$\frac{\partial^2 \varepsilon_\theta}{\partial r^2} + \frac{1}{r^2}\frac{\partial \varepsilon_r}{\partial \theta^2} + \frac{2}{r}\frac{\partial \varepsilon_\theta}{\partial r} - \frac{1}{r}\frac{\partial \varepsilon_r}{\partial r} = \frac{1}{r}\frac{\partial^2 \varepsilon_{r\theta}}{\partial r \partial \theta} + \frac{1}{r^2}\frac{\partial \varepsilon_{r\theta}}{\partial \theta}. \tag{2.3}$$

The plane stress constitutive equations are

$$\varepsilon_r = \frac{1}{E(r)}(\sigma_r - \nu\sigma_\theta), \quad \varepsilon_\theta = \frac{1}{E(r)}(\sigma_\theta - \nu\sigma_r), \quad \varepsilon_{r\theta} = \frac{2(1+\nu)}{E(r)}\sigma_{r\theta}. \tag{2.4}$$

The specific boundary conditions of the problem shown in Fig. 1 are introduced by considering the uniform stress solution for the homogeneous plate without hole (Sadd, 2009). Actually, we know that the presence of the hole acts to disturb this uniform field but we expect this disturbance to be local in nature. The disturbed field will decrease to zero as we move far away from the hole. Based on this we transform the uniform stress from Cartesian coordinates to polar coordinates; in this way we choose the following far-field conditions

$$\sigma_r(\infty, \theta) = \frac{P}{2}(1 + \cos 2\theta), \quad \sigma_{r\theta}(\infty, \theta) = -\frac{P}{2}\sin 2\theta \tag{2.5}$$

and the stress-free hole conditions in the form

$$\sigma_r(a, \theta) = 0, \quad \sigma_{r\theta}(a, \theta) = 0. \tag{2.6}$$

Furthermore, at the interface (for $r = b$) we assume that the ring and the plate are perfectly bonded together; so we require

$$[\sigma_r(b, \theta)] = 0, \quad [\sigma_{r\theta}(b, \theta)] = 0, \tag{2.7}$$

$$[u_r(b, \theta)] = 0, \quad [u_\theta(b, \theta)] = 0. \tag{2.8}$$

3. Solution to the problem

To solve our problem we use the Airy stress function $\varphi(r, \theta)$; the stress components are

$$\sigma_r = \frac{1}{r}\frac{\partial \varphi(r,\theta)}{\partial r} + \frac{1}{r^2}\frac{\partial^2 \varphi(r,\theta)}{\partial \theta^2}, \quad \sigma_\theta = \frac{\partial^2 \varphi(r,\theta)}{\partial r^2},$$
$$\sigma_{r\theta} = \frac{1}{r^2}\frac{\partial \varphi(r,\theta)}{\partial \theta} - \frac{1}{r}\frac{\partial^2 \varphi(r,\theta)}{\partial r \partial \theta}. \tag{3.1}$$

By taking into account the boundary conditions (2.5) we assume the Airy stress function in the form

$$\varphi(r, \theta) = \varphi_0(r) + \varphi_2(r)\cos(2\theta). \tag{3.2}$$

The compatibility Eq. (2.3) in the regions in which the material is homogeneous

$$\nabla^2\nabla^2\varphi(r,\vartheta)=0. \tag{3.3}$$

Concerning the functional ring, we assume that the variation of Young's modulus is

$$E(r)=E_b\left(\frac{r}{b}\right)^m, \tag{3.4}$$

where m is a real positive number while Poisson's ratio ν is assumed constant and equal to the value of the homogeneous medium. In this region the compatibility conditions (2.3), by substituting (3.2) in (2.4) and assuming (3.4), become

$$\frac{d^4\varphi_0(r)}{dr^4}+\frac{2(1-m)}{r}\frac{d^3\varphi_0(r)}{dr^3}+\frac{(m^2+\nu m-m-1)}{r^2}\frac{d^2\varphi_0(r)}{dr^2} -\frac{(m+1)(m\nu-1)}{r^3}\frac{d\varphi_0(r)}{dr}=0, \tag{3.5}$$

$$\frac{d^4\varphi_2(r)}{dr^4}+\frac{2(1-m)}{r}\frac{d^3\varphi_2(r)}{dr^3}+\frac{(m^2+\nu m-m-9)}{r^2}\frac{d^2\varphi_2(r)}{dr^2} -\frac{(m+1)(m\nu-9)}{r^3}\frac{d\varphi_2(r)}{dr}+\frac{4m(m\nu+\nu m-3)}{r^4}\varphi_2(r)=0. \tag{3.6}$$

4. Homogeneous inner ring

The solution for the case of a homogeneous ring around a hole of a homogeneous plate with different elastic modulus is performed in this section. We assume that elastic moduli are E_a and E_b, respectively in the ring and plate. We introduce the apexes (i) and (o) to indicate respectively the quantities related to the inner region $(a\leqslant r\leqslant b)$ and the outer region $(r\geqslant b)$.

The solution (3.2) of Eqs. (3.5) and (3.6) for $m=0$ assumes, in the outer region, the form

$$\varphi^{(o)}(r,\theta)=(z_1\ln(r)+z_2r^2+z_3r^2\ln(r))P +\left(z_{24}+\frac{z_{23}}{r^2}+z_{21}r^2+z_{22}r^4\right)P\cos2\theta, \tag{4.1}$$

where z_1,z_2,z_3 and $z_{24},z_{23},z_{21},z_{22}$ are suitable constants. For the inner region, taking into account the interface conditions (2.7, 2.8), the solution of Eqs. (3.5) and (3.6) are

$$\varphi^{(i)}(r,\theta)=(\alpha_1\ln(r)+\alpha_2r^2+\alpha_3r^2\ln(r))P +\left(\alpha_{24}+\frac{\alpha_{23}}{r^2}+\alpha_{21}r^2+\alpha_{22}r^4\right)P\cos2\theta. \tag{4.2}$$

The explicit solution is now written, by using Eq. (3.1) and boundary conditions (2.6), (2.7) in terms of the constants $\alpha_2,\alpha_{22},\alpha_{24}$. In the inner region we have

$$\sigma_r^{(i)}=-2\left(\frac{a^2}{r^2}-1\right)P\alpha_2-3\left(\frac{a^6}{r^4}-a^2\right)P\alpha_{22}\cos2\theta +\left(\frac{3a^2}{r^4}-\frac{4}{r^2}+\frac{1}{a^2}\right)P\alpha_{24}\cos2\theta,$$

$$\sigma_\theta^{(i)}=2\left(\frac{a^2}{r^2}+1\right)P\alpha_2+3\left(\frac{a^6}{r^4}-a^2+4r^2\right)P\alpha_{22}\cos2\theta -\left(\frac{3a^2}{r^4}+\frac{1}{a^2}\right)P\alpha_{24}\cos2\theta,$$

$$\sigma_{r\theta}^{(i)}=3\left(2r^2-\frac{a^6}{r^4}-a^2\right)P\alpha_{22}\sin2\theta+\left(\frac{3a^2}{r^4}-\frac{2}{r^2}-\frac{1}{a^2}\right)P\alpha_{24}\sin2\theta, \tag{4.3}$$

$$u_r^{(i)}=-\frac{2P}{E_b}\left((\nu-1)r-\frac{(\nu+1)a^2}{r}\right)\alpha_2 +\frac{P}{E_a}\left(\frac{(\nu+1)r}{a^2}+\frac{4}{r}-\frac{(\nu+1)a^2}{r^3}\right)\alpha_{24}\cos2\theta -\frac{P}{E_a}\left(4\nu r^3-3(\nu+1)a^2r-\frac{(\nu+1)a^6}{r^3}\right)\alpha_{22}\cos2\theta,$$

$$u_\theta^{(i)}=\frac{P}{E_a}\left(2(\nu+3)r^3-3(\nu+1)a^2r+\frac{(\nu+1)a^6}{r^3}\right)\alpha_{22}\sin2\theta -\frac{P}{E_a}\left(\frac{(\nu+1)r}{a^2}-\frac{2(\nu-1)}{r}+\frac{(\nu+1)a^2}{r^3}\right)\alpha_{24}\sin2\theta. \tag{4.4}$$

In the outer region we have

$$\sigma_r^{(o)}=\frac{P}{2}\left(1-\frac{b^2}{r^2}\right)+\frac{P}{2}\left(1-\frac{4b^2}{r^2}+\frac{3b^4}{r^4}\right)\cos2\theta-\frac{2P\left(a^2-b^2\right)}{r^2}\alpha_2 +\left(\frac{12b^2\left(a^2-b^2\right)}{r^2}-\frac{3\left(a^6+3a^2b^4-4b^6\right)}{r^4}\right)P\alpha_{22}\cos2\theta -\left(\frac{4(a^2-b^2)}{r^2a^2}-\frac{3(a^4-b^4)}{r^4a^2}\right)P\alpha_{24}\cos2\theta,$$

$$\sigma_\theta^{(o)}=\frac{P}{2}\left(1+\frac{b^2}{r^2}\right)-\frac{P}{2}\left(1+\frac{3b^4}{r^4}\right)\cos2\theta+\frac{2P\left(a^2-b^2\right)}{r^2}\alpha_2 -\frac{3(a^4-b^4)}{r^4a^2}P\alpha_{24}\cos2\theta+\frac{3\left(a^6+3a^2b^4-4b^6\right)}{r^4}P\alpha_{22}\cos2\theta,$$

$$\sigma_{r\theta}^{(o)}=-\left(\frac{1}{2}+\frac{b^2}{r^2}-\frac{3b^4}{2r^4}\right)P\sin2\theta +\left(-\frac{2(a^2-b^2)}{a^2r^2}+\frac{3(a^4-b^4)}{a^2r^4}\right)P\alpha_{24}\sin2\theta +\left(\frac{6b^2(a^2-b^2)}{r^2}-\frac{3\left(a^6+3a^2b^4-4b^6\right)}{r^4}\right)P\alpha_{22}\sin2\theta, \tag{4.5}$$

$$u_r^{(o)}=\frac{((1-\nu)r^2+(1+\nu))b^2P}{2E_br}+\frac{\left((1+\nu)r^4+4b^2r^2-(1+\nu)b^4\right)}{2E_br^3} P\cos2\theta+\frac{2(1+\nu)\left(a^2-b^2\right)}{E_br}P\alpha_2 +\frac{\left(a^2-b^2\right)\left((1+\nu)(a^2+b^2)a^2-12b^2r^2+4b^4(1+\nu)\right)}{E_br^3} P\alpha_{22}\cos2\theta-\frac{\left(a^2-b^2\right)\left((1+\nu)\left(a^2+b^2\right)-4r^2\right)}{E_br^3a^2}P\alpha_{24}\cos2\theta,$$

$$u_\theta^{(o)}=-\frac{\left(\left(b^4+r^4-2b^2r^2\right)\nu+b^4+r^4+2b^2r^2\right)}{2E_br^3}P\sin2\theta+\frac{\left(a^2-b^2\right)\left(\left(4b^4+a^4-6b^2r^2+a^2b^2\right)\nu+4b^4+a^4+6b^2r^2+a^2b^2\right)}{E_br^3}P\alpha_{22} \times\sin2\theta-\frac{(a-b)(a+b)\left(\left(a^2-2r^2+b^2\right)\nu+a^2+2r^2+b^2\right)}{E_br^3a^2}P\alpha_{24}\sin2\theta. \tag{4.6}$$

The remaining constants $\alpha_2, \alpha_{22}, \alpha_{24}$ are obtained by imposing the interface conditions on the displacement (2.8). So doing we get

$$\alpha_2 = -\frac{E_a b^2}{2\left(\left(\left(b^2-a^2\right)\nu - b^2 - a^2\right)E_b - \left(b^2-a^2\right)(\nu+1)E_a\right)}, \quad (4.7)$$

$$\alpha_{22} = \frac{2E_a a^2 b^2\left(a^2-b^2\right)(\nu+1)(E_a-E_b)}{\Omega},$$
$$\alpha_{24} = \frac{2E_a a^2 b^2\left(\left((\nu-3)b^6 - (\nu+1)a^6\right)E_b + \left(a^6-b^6\right)(\nu+1)E_a\right)}{\Omega}, \quad (4.8)$$

$$\begin{aligned}\Omega = {} & (\nu+1)(\nu-3)\left(a^2-b^2\right)^4 E_a^2 \\ & - \left(3(a^4-b^4)^2 + 4b^2a^2(a^4+3b^4)\right)E_b^2 \\ & + \left(\left(a^2-b^2\right)^4\nu^2 - 2\left(a^2-b^2\right)\left(a^6-b^6+5a^4b^2-b^4a^2\right)\nu\right)E_b^2 \\ & + \left(2\left(a^2-b^2\right)^4(1-\nu)\nu + 2\left(a^2-b^2\right)\left(a^6+5b^2a^4-a^2b^4-b^6\right)\nu\right)E_aE_b \\ & + 2\left(a^2-b^2\right)\left(5b^6+5a^2b^4-b^2a^4+3a^6\right)E_aE_b. \end{aligned} \quad (4.9)$$

In order to investigate the hoop stress near the hole we introduce the following quantities

$$K_a^{(HM)} = \frac{\sigma_\theta^{(i)}(a,\pi/2)}{P} = 4\left(\alpha_2 - 3a^2\alpha_{22} + \frac{\alpha_{24}}{a^2}\right). \quad (4.10)$$

For an isotropic homogeneous plate we obtain the SCF by putting $\alpha_2 = 1/4$, $\alpha_{22} = 0$ and $\alpha_{24} = a^2/2$. Furthermore, we consider the normalized hoop stress at the interface in the form

$$K_b^{(HM)} = \frac{\sigma_\theta^{(i)}(b,\pi/2)}{P} = \left(3 - 2\alpha_2\left(1-\frac{a^2}{b^2}\right) - 3\frac{\alpha_{24}}{a^2}\left(1-\frac{a^4}{b^4}\right) + 3\alpha_{22}\left(4b^2 - 3a^2 - \frac{a^6}{b^4}\right)\right). \quad (4.11)$$

Actually, the decrease of Young's modulus in the inner ring with respect to the value of the entire plate leads to an increase of the hoop stress at the interface (for $r = b$). For this reason, if $K_a^{(HM)} > K_b^{(HM)}$, the SCF is at the rim of the hole, while on the other hand, if $K_a^{(HM)} < K_b^{(HM)}$ the SCF occurs at the interface between the rim of the hole and the plate. Numerical investigations will be performed in Section 6.

5. FGM inner ring solution

The solution for the stress function in an FGM inner ring is obtained by solving compatibility Eqs. (3.5) and (3.6). The solution (3.2) becomes

$$\begin{aligned}\varphi^{(FG)}(r,\theta) = {} & \left(C_1 r^{m/2+\rho/2+1} + C_2 r^{m/2-\rho/2+1}\right)P + r^{m+1}(D_1A_1(r) \\ & + D_2A_2(r) + D_3B_1(r) + D_4B_2(r))P\cos 2\theta, \end{aligned} \quad (5.1)$$

where

$$\begin{aligned} & A_1(r) = r^{-m/2-\alpha/2}, \quad A_2(r) = r^{-m/2+\alpha/2}, \\ & B_1(r) = r^{-m/2-\beta/2}, \quad B_2(r) = r^{-m/2+\beta/2} \end{aligned} \quad (5.2)$$

and $C_1, C_2, D_1, D_2, D_3, D_4$ are constants to be found. We have also set

$$\begin{aligned} & \alpha = \sqrt{m^2+2m-2\nu m+20-2\sqrt{m^2+\nu^2m^2-14\nu m^2-32\nu m+32m+64}}, \\ & \beta = \sqrt{m^2+2m-2\nu m+20+2\sqrt{m^2+\nu^2m^2-14\nu m^2-32\nu m+32m+64}}, \\ & \rho = \sqrt{m^2+4-4\nu m}. \end{aligned} \quad (5.3)$$

Depending on the specific values of m and ν, the coefficients α, β can assume real or complex values. In this work we assume that m is in the range

$$0 \leqslant m \leqslant \frac{8(2-\sqrt{3})}{\nu - 7 + 4\sqrt{3}}. \quad (5.4)$$

This assumption, which is true for many cases of applicative interest, ensures that α and β are real (see also Section 6).

The stress and displacement fields, in the inner FG region, are

$$\begin{aligned}\sigma_r^{(FG)} = {} & \frac{(m+\rho+2)r^{m/2+\rho/2}C_1 + (m-\rho+2)r^{m/2-\rho/2}C_2}{2r} \\ & P + \frac{(m-\alpha-6)A_1(r)D_1 + (m-\beta-6)B_1(r)D_3}{2r^{1-m}} \\ & P\cos 2\theta + \frac{(m+\beta-6)B_2(r)D_4 + (m+\alpha-6)A_2(r)D_2}{2r^{1-m}} \\ & P\cos 2\theta, \end{aligned}$$

$$\begin{aligned}\sigma_\theta^{(FG)} = {} & \frac{(m+\rho)(m+\rho+2)r^{m/2+\rho/2}C_1 + (m-\rho)(m-\rho+2)r^{m/2-\rho/2}C_2}{4r} \\ & P + \frac{(m-\alpha)(m-\alpha+2)A_1(r)D_1 + (m-\beta)(m-\beta+2)B_1(r)D_3}{4r^{1-m}} \\ & P\cos 2\theta + \frac{(m+\beta)(m+\beta+2)B_2(r)D_4 + (m+\alpha)(m+\alpha+2)A_2(r)D_2}{4r^{1-m}} \\ & P\cos 2\theta, \end{aligned}$$

$$\sigma_{r\theta}^{(FG)} = \frac{(m-\alpha)A_1(r)D_1 + (m-\beta)B_1(r)D_3 + (m+\beta)B_2(r)D_4 + (m+\alpha)A_2(r)D_2}{r^{1-m}} P\sin 2\theta,$$

$$\begin{aligned}u_r^{(FG)} = {} & \frac{\left(m^2 + (1+\rho-3\nu)m - (\rho+2)(\nu-1)\right)r^{-m/2+\rho/2}b^m C_1}{2E_b} \\ & P + \frac{\left(m^2 + (1-\rho-3\nu)m + (\rho-2)(\nu-1)\right)r^{-m/2-\rho/2}b^m C_2}{2E_b} \\ & P + \frac{M_{13}B_1(r)D_3 + M_{14}B_2(r)D_4 + M_{11}A_1(r)D_1 + M_{12}A_2(r)D_2}{E_b} b^m \\ & P\cos 2\theta, \end{aligned}$$

$$u_\theta^{(FG)} = -\frac{M_{24}A_1(r)D_1 + M_{22}A_2(r)D_2 + M_{23}B_2(r)D_4 + M_{21}B_1(r)D_3}{E_b} b^m P\sin 2\theta, \quad (5.5)$$

where the quantities $M_{11}, M_{12}M_{13}, M_{14}, M_{21}, M_{22}, M_{23}, M_{24}$ are coefficients depending on m and ν (see Appendix).

For the outer homogeneous region we assume the stress function in the form (4.1) and we obtain

$$\begin{aligned} \sigma_r^{(o)} &= P\left(\frac{1}{2} + \frac{z_1}{r^2}\right) + \left(\frac{1}{2} - \frac{4z_{24}}{r^2} - \frac{6z_{23}}{r^4}\right)P\cos 2\theta, \\ \sigma_\theta^{(o)} &= P\left(\frac{1}{2} - \frac{z_1}{r^2}\right) - \left(\frac{1}{2} - \frac{6z_{23}}{r^4}\right)P\cos 2\theta, \\ \sigma_{r\theta}^{(o)} &= -\left(\frac{1}{2} + \frac{2z_{24}}{r^2} + \frac{6z_{23}}{r^4}\right)P\sin 2\theta, \\ u_r^{(o)} &= \frac{(1-\nu)Pr}{2E_b} - \frac{(1+\nu)Pz_1}{E_b r} + \frac{1}{E_b}\left(\frac{(1+\nu)r}{2} + \frac{4z_{24}}{r} + \frac{2(1+\nu)z_{23}}{r^3}\right) \\ & \quad P\cos 2\theta, \\ u_\theta^{(o)} &= -\frac{(1+\nu)}{E_b}\left(\frac{r}{2} + \frac{z_{24}}{r} - \frac{2z_{23}}{r^3}\right)P\sin 2\theta. \end{aligned} \quad (5.6)$$

By using boundary and interface conditions (2.5)–(2.8) we are able to explicitly write the constants $D_1, D_2, D_3, D_4, C_1, C_2$ for the inner region and z_1, z_{23}, z_{24} for the solution in the outer region (see Appendix). The behavior of the stress components will be investigated in the next section.

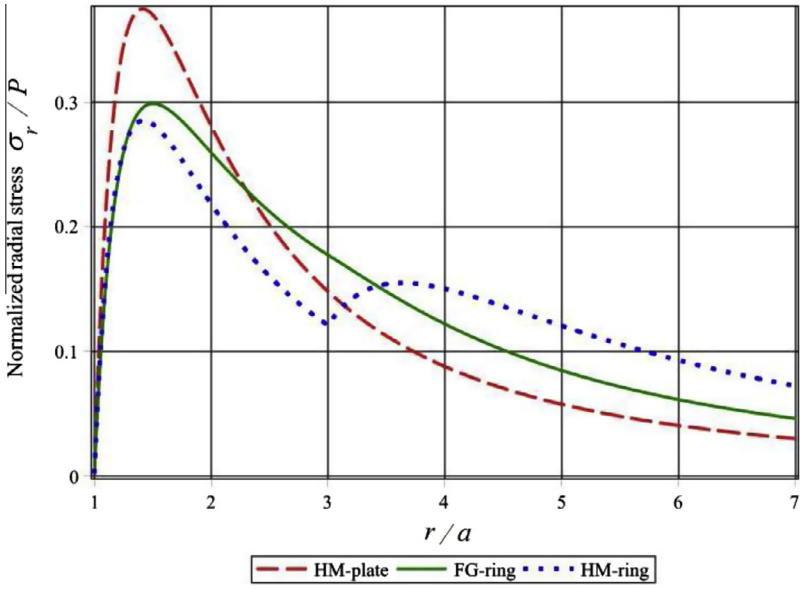

Fig. 2. Normalized radial stress in the radial direction for $\theta = \pi/2$ ($\nu = 0.3$).

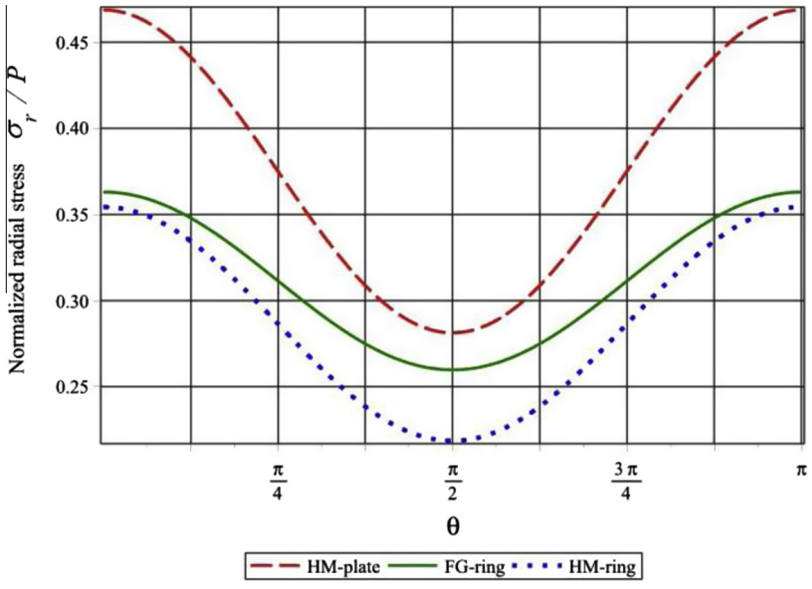

Fig. 3. Angular variation of the normalized radial stress for $r = 2a$.

In a similar way as the previous Section 4 for homogeneous ring, we introduce the following quantities

$$K_a^{(FG)} = \frac{\sigma_\theta^{(FG)}(a,\pi/2)}{P} = \frac{(m+\rho+2)(m-\rho+2)\rho a^{m/2-\rho/2} b^{-m/2+1}}{2a(1+\nu)m\left((m+\rho+2)a^{-\rho}b^{\rho/2} - (m-\rho+2)b^{-\rho/2}\right)} + \frac{(\beta-\alpha)a^{m/2}}{2a}\left(\alpha a^{-\alpha/2}D_1 - \beta a^{\beta/2}D_4\right). \tag{5.7}$$

We remark that this expression assumes the conventional SCF value for a homogeneous plate by assuming $a = b$ or $m = 0$. Furthermore, we define the quantities

$$K_b^{(FG)} = \frac{\sigma_\theta^{(FG)}(b,\pi/2)}{P} = 1 - \frac{6z_{23}}{b^4} - \frac{z_1}{b^2}. \tag{5.8}$$

If $K_a^{(FG)} > K_b^{(FG)}$, the SC is at the rim of the hole, instead if $K_a^{(FG)} < K_b^{(FG)}$ the SCF occurs at the interface. Numerical investigations will be performed in Section 6.

6. Numerical results

In this section numerical results are obtained to optimize the graded elastic properties of the ring in order to reduce SCF in the entire homogeneous plate. We compare the two solutions presented in Sections 4 and 5 for a homogeneous ring (HM-ring) and a functionally graded ring (FG-ring); furthermore, we compare

the numerical results with those obtained for a homogeneous plate with hole (HM-plate) by assuming $E = E_b$.

In the numerical example we take $b/a = 3$, $m = 0.5$ ($E_a \cong 0.57E_b$), $\nu = 0.3$. In Fig. 2 the behavior of the normalized radial stress σ_r/P in the thickness of the plate for $\theta = \pi/2$ is presented; the maximum value occurs in the ring and decreases with respect to the homogeneous case. The normalized radial stress for $r = 2a$ in terms of the angular distribution is shown in Fig. 3 and presents a reduction of the maximum value in the ring in comparison with the homogeneous stiffener plate. In Fig. 4 the normalized hoop stress σ_θ/P in the thickness of the plate at $\theta = \pi/2$ is shown; we observe the reduction of the stress value at the rim of the hole (SCF) due to the graded properties and the continuity of the stress on the interface in comparison with the homogeneous ring. In Fig. 5 the normalized hoop stress in the rim of the circular hole ($r = a$) in terms of the angular distribution shows that the reduction of the stress is comparable with the reduction obtained by using HM ring but the gap on the interface is fully avoided by using material inhomogeneity. In Fig. 6 the normalized tangential stress $\sigma_{r\theta}/P$ is shown for $\theta = \pi/4$; the variation with the angular distribution is shown in Fig. 7 for $r = 2a$.

Then, in Fig. 8, by considering $b/a = 3$, $\nu = 0.3$, $\theta = \pi/2$ and different values of m in the range ($0 \leqslant m \leqslant 9$) we plot the hoop stress in the radial direction. We observe that the maximum value of hoop stress is no longer necessarily in the inner part of the ring $r = a$ as in the homogeneous case. As m increases, one observes from Fig. 8 that $K_a^{(FG)}$ decreases while $K_b^{(FG)}$ increases. For this reason the aim to minimize the hoop stress to prevent failure cannot take into account only the value in $r = a$. A numerical analysis can be done to find the value of m for which one obtains the choice $m = \tilde{m}$ where $K_a^{(FG)} = K_b^{(FG)}$ (see Eqs. (5.7) and (5.8)). In our numerical case this condition gives $\tilde{m} \cong 1.10$ corresponding to $E_a/E_b \cong 0.30$. For values of $m < \tilde{m}$ we have $K_a^{(FG)} < K_b^{(FG)}$ and so the hoop stress has its maximum value for $r = a$. For values of $m > \tilde{m}$ we have $K_a^{(FG)} > K_b^{(FG)}$ and the maximum hoop stress occurs at the interface $r = b$.

In a similar way, for the homogeneous ring case, with two different Young's moduli E_a and E_b related by equation:

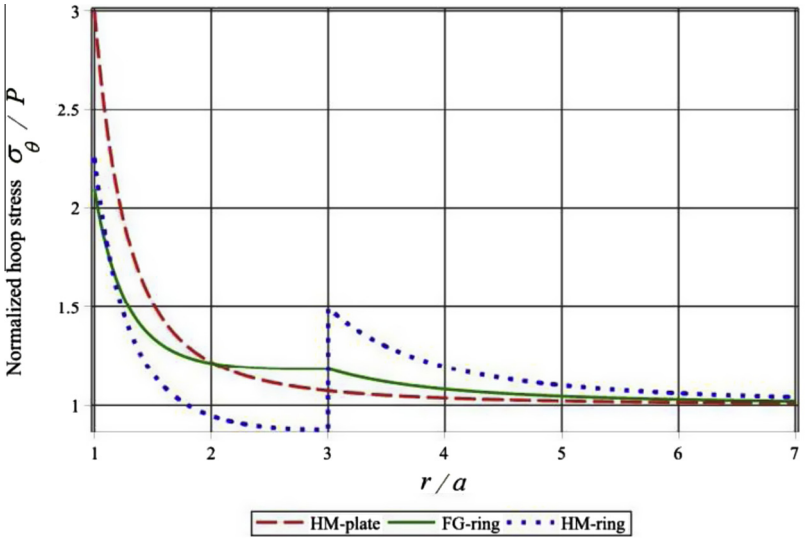

Fig. 4. Normalized hoop stress in the radial direction for $\theta = \pi/2$ ($\nu = 0.3$).

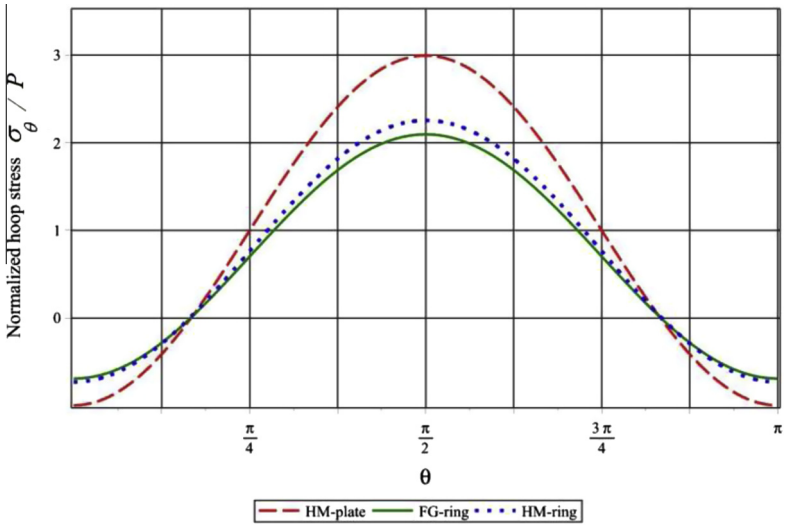

Fig. 5. Angular variation of the normalized hoop stress on the rim of the circular hole.

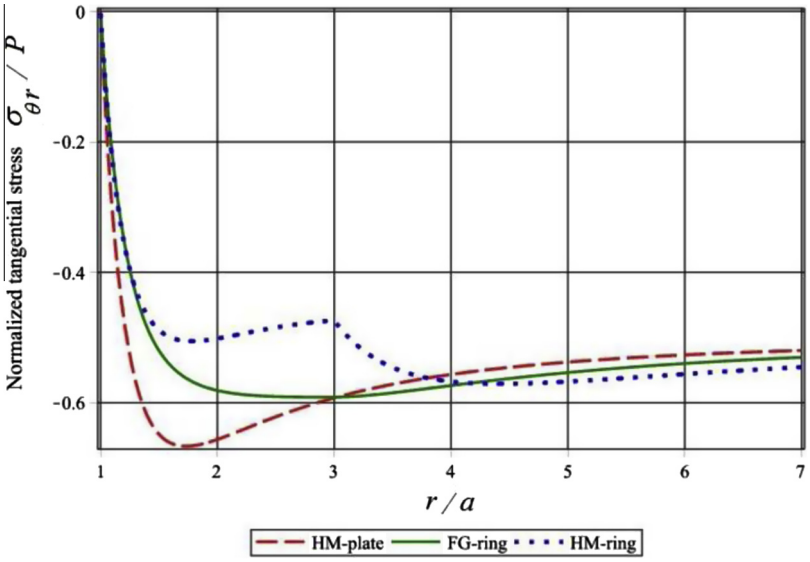

Fig. 6. Normalized tangential stress in the radial direction for $\theta = \pi/4$ ($\nu = 0.3$).

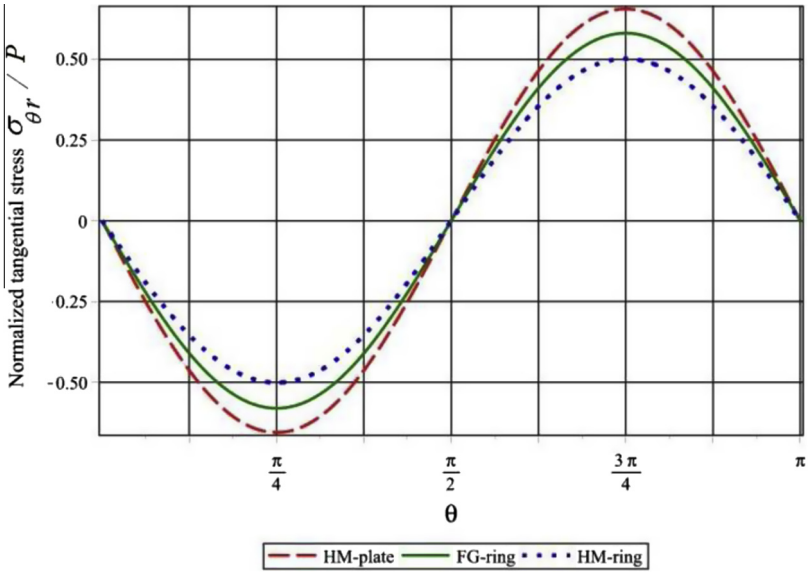

Fig. 7. Angular variation of the normalized tangential stress for $r = 2a$.

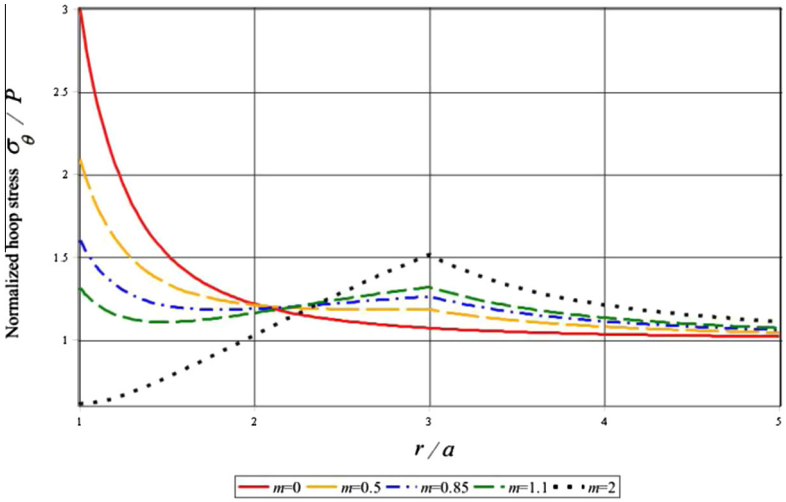

Fig. 8. Normalized hoop stress in radial direction for different inhomogeneity parameter m in plate with FGM ring ($b = 3a, \theta = \pi/2, \nu = 0.3$).

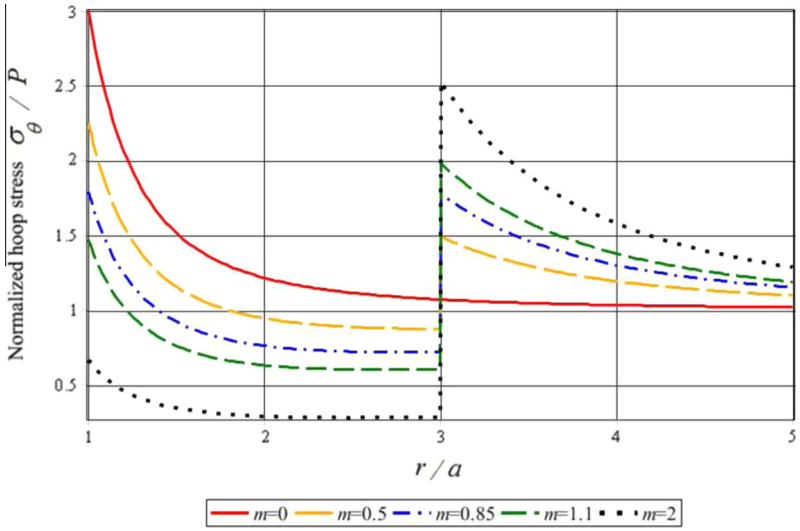

Fig. 9. Normalized hoop stress in radial direction for different m values in plate with HM ring ($b = 3a, \theta = \pi/2, \nu = 0.3$).

$E_a/E_b = (a/b)^m$, in Fig. 9 we plot the normalized hoop stress in the radial direction for different values of m. At the interface we observe the gap due to the mismatch of the material; as $K_a^{(HM)}$ decreases, $K_b^{(HM)}$ increases and the gap at the interface increases. The corresponding value of $m = \hat{m}$ where $K_a^{(HM)} = K_b^{(HM)}$ (see Eqs. (4.10) and (4.11)) occurs for $\hat{m} = 0.85$ corresponding to a ratio $E_a/E_b \cong 0.39$.

7. Concluding remarks

In this paper analytical solutions in closed form useful to investigate the effects of material inhomogeneity, to reduce SCF around a hole of a homogeneous plate, are obtained. Numerical results and comparisons with solutions for a conventional homogeneous material inner ring can be helpful to material scientists in order to design new materials according to the required performances. The conclusions from the parametric study are the following:

1. A required reduction in the SCF of the entire homogeneous plate can be obtained with FGM ring in which Young's modulus progressively increases away from the center of the hole in an optimized way.
2. The stress concentration variation depends only on the inhomogeneity parameter m and the ratio b/a.
3. Numerical comparisons with the solution for a homogeneous ring permit us to show that the SCF is less influenced by the variation of Poisson's ratio.

Thus, the explicit solutions obtained allow us to better describe a compositional variation of the elastic properties near the holes in the thickness of the annular ring; compositional variations that, if optimized, can lead to increase the load bearing capacity in the plate (see, for example Götzen et al., 2003; Venkataraman et al., 2003).

Acknowledgments

Work financed by the Italian Ministry of Education, University and Research (MIUR). Project No. 2009XWLFKW: "Multi-scale modeling of materials and structures".

Appendix A

We write the coefficient and constant values for the FGM ring case.

$$M_{11} = \frac{(m^2 + 2(1-\alpha)m - \alpha(2-\alpha))\nu}{2(m+\alpha)} - \frac{m-\alpha-6}{m+\alpha},$$
$$M_{12} = \frac{(m^2 + 2(\alpha+1)m + \alpha(2+\alpha))\nu}{2(m-\alpha)} - \frac{m+\alpha-6}{m-\alpha},$$
$$M_{13} = \frac{(m^2 + 2(1-\beta)m - \beta(2-\beta))\nu}{2(m+\beta)} - \frac{m-\beta-6}{m+\beta},$$
$$M_{14} = \frac{(m^2 + (2\beta+2)m + \beta(2+\beta))\nu}{2(m-\beta)} - \frac{m+\beta-6}{m-\beta},$$

$$M_{21} = \frac{1}{96}\left(m^2(4\nu-28) + m(\beta^2 - \alpha^2 + 28\beta - 4\beta\nu - 24\nu - 88)\right) + \frac{1}{96}\left(-\beta^3 - 6\beta^2 + 6\alpha^2 + \alpha^2\beta + 64\beta - 192\nu - 192\right), \tag{8.1}$$

$$M_{22} = \frac{1}{96}\left(m^2(4\nu-28) + m(\alpha^2 - \beta^2 - 28\alpha + 4\alpha\nu - 24\nu - 88)\right) + \frac{1}{96}\left(\alpha^3 - 6\alpha^2 + 6\beta^2 - \beta^2\alpha - 64\alpha - 192\nu - 192\right),$$
$$M_{23} = \frac{1}{96}\left(m^2(4\nu-28) - m(\alpha^2 - \beta^2 + 28\beta - 4\beta\nu + 24\nu + 88)\right) - \frac{1}{96}\left(-\beta^3 + 6\beta^2 - 6\alpha^2 + \alpha^2\beta + 64\beta + 192\nu + 192\right),$$
$$M_{24} = \frac{1}{96}\left(m^2(4\nu-28) - m(\beta^2 - \alpha^2 - 28\alpha + 4\alpha\nu + 24\nu + 88)\right) - \frac{1}{96}\left(\alpha^3 - 6\beta^2 + 6\alpha^2 - \beta^2\alpha - 64\alpha + 192\nu + 192\right).$$

Furthermore, we have

$$z_1 = -\frac{b^2}{2} + \frac{b^2(m-\rho+2)\left(b^{\rho/2} - b^{-\rho/2}a^\rho\right)(m+2+\rho)}{2m(1+\nu)\left((m+\rho+2)b^{\rho/2} - (m-\rho+2)a^\rho b^{-\rho/2}\right)}, \tag{8.2}$$

and

$$z_{23} = -\frac{b^4}{4} - \frac{b^{m+3}(m+\beta+2)B_2(b)}{4}D_4 - \frac{b^{m+3}(m-\alpha+2)A_1(b)}{4}D_1 + \frac{b^{m+3}((m-\beta+2)(\alpha-\beta)A_2(a)B_1(b)+2\beta(m+\alpha+2)A_2(b)B_1(a))B_2(a)}{4(\alpha+\beta)B_1(a)A_2(a)}D_4 + \frac{b^{m+3}(-(m+\alpha+2)(\alpha-\beta)A_2(b)B_1(a)+2\alpha(m-\beta+2)A_2(a)B_1(b))A_1(a)}{4(\alpha+\beta)B_1(a)A_2(a)}D_1, \tag{8.3}$$

$$z_{24} = \frac{b^2}{2} + b^{m+1}\frac{(m-\alpha+6)A_1(b)}{4}D_1 + b^{m+1}\frac{(m+\beta+6)B_2(b)}{4}D_4 + b^{m+1}\left(\frac{(\alpha-\beta)(m+\alpha+6)A_1(a)A_2(b)}{4(\alpha+\beta)A_2(a)} - \frac{\alpha(m-\beta+6)A_1(a)B_1(b)}{2(\alpha+\beta)B_1(a)}\right)D_1 - b^{m+1}\left(\frac{(\alpha-\beta)(m-\beta+6)B_1(b)B_2(a)}{4(\alpha+\beta)B_1(a)} + \frac{\beta(m+\alpha+6)A_2(b)B_2(a)}{2(\alpha+\beta)A_2(a)}\right)D_4 \tag{8.4}$$

$$C_1 = \frac{(m-\rho+2)a^{-\rho}b^{1-m/2}}{(1+\nu)m\left((m+\rho+2)a^{-\rho}b^{\rho/2} - (m-\rho+2)b^{-\rho/2}\right)}, \qquad C_2 = -\frac{(m+2+\rho)b^{1-m/2}}{(1+\nu)m\left((m+\rho+2)a^{-\rho}b^{\rho/2} - (m-\rho+2)b^{-\rho/2}\right)}. \tag{8.5}$$

Finally we get

$$D_2 = -\frac{2\beta B_2(a)}{(\alpha+\beta)A_2(a)}D_4 + \frac{(\alpha-\beta)A_1(a)}{(\alpha+\beta)A_2(a)}D_1, \quad D_1 = \frac{D_{11}}{\Lambda}, \qquad D_3 = -\frac{(\alpha-\beta)B_2(a)}{(\alpha+\beta)B_1(a)}D_4 - \frac{2\alpha A_1(a)}{(\alpha+\beta)B_1(a)}D_1 \quad D_4 = \frac{D_{44}}{\Lambda}, \tag{8.6}$$

where

$$D_{11} = 4bb^m\beta(\alpha+\beta)((m+\alpha-2)(1+\nu)+2M_{12}-2M_{22})A_2(a)A_2(b)^2B_2(b)B_2(a) + 2a^m b(\alpha^2-\beta^2)((m-\beta-2)(1+\nu)+2M_{13}-2M_{21})A_2(b)A_2(a)^2B_2(a)^2 - 2bb^m(\alpha+\beta)^2((m+\beta-2)(1+\nu)+2M_{14}-2M_{23})A_2(b)A_2(a)^2B_2(b)^2,$$

$$D_{44} = -4b\alpha(\alpha+\beta)((m-\beta-2)(1+\nu) + 2M_{13}-2M_{21})A_2(a)A_2(b)B_2(a) + 2a^{-m}bb^m(\alpha^2-\beta^2)((m+\alpha-2)(1+\nu) + 2M_{12}-2M_{22})A_2(b)^2B_2(b) + 2b(\alpha+\beta)^2((m-\alpha-2)(1+\nu) + 2M_{11}-2M_{24})A_2(a)^2B_2(b), \tag{8.7}$$

$$\Lambda = \lambda_1 b^{2m}a^{-m}A_2(b)^2B_2(b)^2 + \lambda_2 b^m A_2(b)^2B_2(a)^2 + \lambda_3 b^m A_2(a)A_2(b)B_2(a)B_2(b) + \lambda_4 b^m A_2(a)^2B_2(b)^2 + \lambda_5 a^m A_2(a)^2B_2(a)^2 \tag{8.8}$$

and the coefficients λ_i are in terms of m and ν in the following form

$$\lambda_1 = 2(\alpha^2-\beta^2)((m+\alpha+4-2\nu-M_{22})M_{14} - (m+\beta+4-2\nu-M_{23})M_{12}) + (\alpha^2-\beta^2)(((m+\alpha+2)\nu-m-\alpha-10)M_{23} - ((m+\beta+2)\nu-m-\beta-10)M_{22}) + 2(\alpha-\beta)^2(\alpha+\beta)(1+\nu)(\nu-3),$$

$$\lambda_2 = (\alpha+\beta)^2(((m-\beta+2)\nu-m+\beta-10+2M_{13})M_{22} - 2(m+\alpha+4-2\nu)M_{13}) + (\alpha+\beta)^2(2(m-\beta+4-2\nu-M_{21})M_{12} - ((m+\alpha+2)\nu-m-\alpha-10)M_{21}) - 2(\alpha+\beta)^3(1+\nu)(\nu-3),$$

$$\lambda_3 = 2\alpha(\alpha+\beta)(2(m+\beta+4-2\nu-M_{23})M_{13} - ((m-\beta+2)\nu-m+\beta-10)M_{23}) + 2\beta(\alpha+\beta)(2(m+\alpha+4-2\nu-M_{22})M_{11} - ((m-\alpha+2)\nu-m+\alpha-10)M_{22}) + 2(\alpha+\beta)\beta((m+\alpha+2)\nu-m-\alpha-10+2M_{12})M_{24} + 2\alpha(\alpha+\beta)((m+\beta+2)\nu-m-\beta-10+2M_{14})M_{21} - 4(\alpha+\beta)((m-\beta+4-2\nu)\alpha M_{14} + (m-\alpha+4-2\nu)\beta M_{12} - 4\alpha\beta(1+\nu)(\nu-3)),$$

$$\lambda_4 = 2(\alpha+\beta)^2((m-\alpha+4-2\nu-M_{24})M_{14} - (m+\beta+4-2\nu-M_{23})M_{11}) + (\alpha+\beta)^2(((m-\alpha+2)\nu + \alpha-m-10)M_{23} - ((m+\beta+2)\nu-m-\beta-10)M_{24}) - 2(\alpha+\beta)^3(1+\nu)(\nu-3),$$

$$\lambda_5 = (\alpha^2-\beta^2)(2(m-\beta+4-2\nu-M_{21})M_{11} - ((m-\alpha+2)\nu-m+\alpha-10)M_{21}) + (\alpha^2-\beta^2)(2(-m+\alpha-4+2\nu+M_{24})M_{13} + ((m-\beta+2)\nu-m+\beta-10)M_{24}) + 2(\alpha-\beta)^2(\alpha+\beta)(1+\nu)(\nu-3). \tag{8.9}$$

References

Artioli, E., Bisegna, P., Maceri, F., 2010. Effective longitudinal shear moduli of periodic fibre-reinforced composites with radially-graded fibres. International Journal of Solids and Structures 47, 383–397.

Batra, R.C., 2011. Material tailoring and universal relations for axysimmetric deformations of functionally graded rubberlike cylinders and spheres. Mathematics and Mechanics of Solids 16, 729–738.

Birman, V., Byrd, L.W., 2007. Modeling and analysis of functionally graded materials and structures. Applied Mechanics Review 60, 195–216.

Buskirk, S.R., Venkataraman, S., Ifju, P.G., Rapoff, A.J., 2002. Functionally graded biomimetic plate with hole. In: SEM Annual Conference & Exposition on Experimental and Applied Mechanics.

Chao, C.K., Lu, L.M., Chen, C.K., Chen, F.M., 2009. Analytical solution for a reinforcement layer bonded to an elliptic hole under a remote uniform load. International Journal of Solids and Structures 46, 2959–2965.

Dryden, J.R., Batra, R.C., 2013. Optimum Young's modulus of a homogeneous cylinder energetically equivalent to a functionally graded cylinder. Journal of Elasticity 110, 95–110.

Götzen, N., Cross, A.R., Ifju, P.G., Rapoff, A., 2003. Understanding stress concentration about a nutrient foramen. Journal of Biomechanics 36 (10), 1511–1521.

Hosseini-Hashemi, Sh., Salehipuor, H., Atashipour, S.R., Sburlati, R., 2013. On the exact in-plane and out-of-plane free vibration analysis of thick functionally

graded rectangular plates: explicit 3-D elastic solutions. Composites Part B: Engineering, Composites: Part B 46 (1), 108–115.
Kashtalyan, M., Menshykova, M., 2008. Three-dimensional analysis of a functionally graded coating/substrate system of finite thickness. Proceedings of the Royal Society: A 366, 1821–1826.
Kubair, D.V., Bhanu-Chandar, B., 2008. Stress concentration factor due to a circular hole in functionally graded panels ander uniaxial tension. International Journal of Mechanical Sciences 50, 732–742.
Lutz, M.P., Zimmerman, R.W., 1996. Effect of the interphase zone on the bulk modulus of a particular composite. ASME, Journal of Applied Mechanics 63, 855–861.
Mohammadi, M., Dryden, J.R., Jiang, L., 2011. Stress concentration around a hole in a radially inhomogeneous plate. International Journal of Solids and Structures 48, 483–491.
Nagpal, S., Jain, N., Sayal, S., 2012. Stress concentration and its mitigation techniques in flat plate with singularities: a critical review. Engineering Journal 16 (1).
Nie, G.J., Batra, R.C., 2010. Exact solutions and material tayloring for functionally graded hollow circular cylinders. Journal of Elasticity 99, 179–201.
Sadd, M.H., 2009. Elasticity, second ed. Academic Press.
Sburlati, R., 2002. The contact behavior between a foam core sandwich plate and a rigid indenter. Composites Part B: Engineering 33, 325–332.
Sburlati, R., 2004. An exact solution for the impact law in thick elastic plates. International Journal of Solids and Structures 41 (9–10), 2539–2550.
Sburlati, R., 2009a. Adhesive elastic contact between a symmetric indenter and elastic film/substrate systems. International Journal of Solids and Structures 46 (5), 975–988.
Sburlati, R., 2009b. Three-dimensional analytical solution for an axisymmetric biharmonic problem. Journal of Elasticity 95 (1–2), 79–97.
Sburlati, R., 2012a. Elastic solution in a functionally graded coating subjected to a concentrated force. Journal of Mechanics of Materials and Structures 7 (4), 401–412.
Sburlati, R., 2012b. Analytical elastic solutions for pressurized hollow cylinders with internal functionally graded coatings. Composite Structures 94 (12), 3592–3600.
Sburlati, R., Atashipour, S.R., Hosseini-Hashemi, Sh., 2013. Study on the effect of functionally graded coating layers on elastic deformation of a thick circular plate: a closed-form elasticity solution. Composite Structure 99 (1), 131–140.
Suresh, S., 2001. Graded materials for resistance to contact deformation and damage. Science 292 (5526), 2447–2451.
Theotokoglou, E.E., Tampouloglou, I.H., 2008. The radially nonhomogeneous elastic axisymmentric problem. International Journal of Solids and Structures 45, 6535–6552.
Venkataraman, S., Haftka, R.T., Rapoff, A.J., 2003. Structural optimization using biological variable to help understand bones design holes. Structural and Multidisciplinary Optimization 25, 19–34.
Yang, Q., Gao, C.F., Chen, W., 2010. Stress analysis of a functionally graded material plate with a circular hole. Archive of Applied Mechanics 80, 895–907.